ANISOTROPY OF HEAT TRANSFER PROCESSES IN A ROTATING FLOW IN A UNIFORM MAGNETIC FIELD WITH NONUNIFORM ELECTRICAL CONDUCTIVITY AT THE BOUNDARIES

O. V. Andreev and Yu. B. Kolesnikov

Anisotropic heat transfer in a rotating turbulent flow in an axially uniform magnetic field is studied experimentally. Heat transfer intensities when a wall perpendicular to the field is nonconducting or has regions of high conductivity are compared. It is shown that inserting a wall with high conductivity leads to a 5-6 times increase in heat transfer. Measurements of local characteristics are used for analyzing the flow structure and the redistribution of the velocity and temperature distributions in these cases.

Introduction. In a number of applied magnetohydrodynamics problems it becomes necessary to intensify heat transfer during certain processes. One efficient method for such intensification may be to excite large-scale two-dimensional vortical structures in a fluid in an external transverse magnetic field. These structures can be excited in two ways. The first method is based on creating highly unstable shear flows in the fluid in crossed electric and magnetic fields [1-3]. The interaction of the current flowing through the liquid with the magnetic field produces a helical electromagnetic force which, for certain distributions of the electric field, forms a nonuniform two-dimensional flow with free shear layers parallel to the magnetic field. As they are highly unstable, these flows generate two-dimensional perturbations whose intensity is as much as 25% of the average energy expenditure. The other method is based on creating conditions for a redistribution of the induced currents in channeled flows by means of a sudden change in the conductivity of walls perpendicular to the magnetic field [4-6]. As a result of shorting of the induced currents at the high-conductivity sections and, therefore, of their nonuniform distribution along the magnetic field, in the region of the discontinuity in the conductivity at the wall a helical component of the electromagnetic force develops which gives rise to vorticity in the field direction. The appearance of this vorticity, in turn, leads to a slowing down of the fluid over the electrically conducting region of the walls. In fact, visual observations of the free surface in experiments with mercury in a pan [6] have demonstrated that in a sufficiently strong magnetic field there is no motion of the fluid above an electrically conducting region.

The possibility of intensifying heat transfer by means of large-scale vortical structures created in a flow by high-conductivity segments located at an insulating channel wall perpendicular to the flow has been confirmed experimentally [7]. As an extension of that work, here we present results from detailed studies of flows of this type: the formation of the velocity and temperature distributions, their fluctuation characteristics, and the intensity and direction of heat transfer.

1. Experimental Apparatus and Measurement Technique. The experiments were done in an annular channel with a rectangular cross section having a height of $2a = 46$ mm (Fig. 1). The outer radius of the channel $R = 60$ cm and the inner radius $r_0 = 27.5$ mm. The 5-mm-thick copper side walls of the channel were parallel to the magnetic field and served as electrodes for passing a constant electric current from a power supply radially through the working fluid. The inner wall of the channel contain an electric heated consisting of a nichrome wire powered by a dc supply. The operating power of the heater was such as to ensure a heat flux through the inner wall of up to 5.9 kW/m^2. The outer wall had a water cooling channel. The temperature of this wall was held constant at 20 ± 0.1°C by a thermostat. The bottom and upper cover of the channel were heat insulated. A magnetic field was created in the channel by a dc electromagnet whose pole pieces were separated by 150 mm. The experiments were carried out at magnetic inductions B = 0.64-1.4 T and electric currents I = 5-30 A.

Translated from Magnitnaya Gidrodinamika, No. 2, pp. 87-94, April-June, 1993. Original article submitted May 17, 1993.

0024-998X/93/2902-0181$12.50

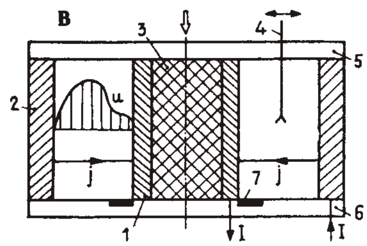

Fig. 1. A sketch of the experimental apparatus: (1) inner and (2) outer electrodes, (3) heater, (4) probe, (5) cover, (6) bottom, (7) copper inserts.

A eutectic In–Ga–Sn alloy with density $\rho = 6400$ kg/m^3, kinematic viscosity $\nu = 34 \cdot 10^{-7}$ m^2/sec, electrical conductivity $\sigma = 3.46 \cdot 10^6$ $\Omega^{-1} \cdot$m^{-1}, and thermal conductivity $\lambda = 39$ W/(m·deg) at T = 20°C was used as a working fluid.

The fluid moved in the channel because of the interaction of the radial component of the electric current with a uniform external vertical magnetic field. The cylindrical geometry of the apparatus and the symmetric external current input to the side walls of the channel ensured that the distribution of the radial electric current density in the channel was uniform and, therefore, that the azimuthal distribution of the electromagnetic force $\mathbf{j} \times \mathbf{B}$ was also uniform. In this type of flow there is no longitudinal pressure gradient along the flow and there are none of the end effects characteristic of channels with inlet and outlet sections.

In order to produce the most efficient flow turbulence from the standpoint of intensifying heat transfer, 8-mm-thick and 5-mm-wide copper inserts separated by 40° were placed in the bottom of the channel. In the first series of experiments the inserts were 5 mm long and mounted a distance of 5 mm from the heated wall. In the second series the inserts were 11 mm long and positioned with their long edge along the channel radius at the heated wall (Fig. 1).

The mean azimuthal velocity and temperature, radial component of the velocity fluctuations, and temperature fluctuations were measured. The velocity characteristics were measured using a conduction anemometer with a four-electrode probe. The probe electrodes were made of 0.33-mm-diameter insulated copper wire. The ends of the electrodes were in contact with the liquid and were located immediately at the measurement point and separated by 1.2 mm from one another. The probe case consisted of an insulated copper tube with an outer diameter of 2 mm. The overall length of the probe was 23 mm, i.e., the measurement point was located in the midplane of the channel. The anemometer probe was moved radially, transversely to the channel (Fig. 1). The accuracy of the scale on the specially made positioner was 0.1 mm.

An induction method for measuring the velocity was chosen because the flow of the liquid metal at the magnetic fields used in these experiments is essentially two-dimensional, as found elsewhere [1-3]. If we define

$$\varepsilon = \left[(2a)^{-1} \int_{-a}^{a} (1 - vB/E)^2 dz \right]^{1/2}$$

as the root mean square relative error in the velocity measured by the conduction anemometer in a two-dimensional flow of height $2a$ (here E is the electric field strength in a plane perpendicular to the magnetic field measured by the anemometer and B is the magnetic induction), then ε for the actual fluid velocity can be estimated using Hartmann's solution for the velocity profile (in relative units),

$$v = (2Ba)^{-1}[(\mathrm{Ha} - \mathrm{th\,Ha})/(\mathrm{th\,Ha} + \alpha\,\mathrm{Ha})]$$

(where α is the relative conductivity of the wall perpendicular to the field) and the corresponding expression for the electric field

$$E = vB[\mathrm{Ha}/(\mathrm{Ha} - \mathrm{th\,Ha})].$$

For an unconfined flow excited by the interaction of the electric current with the magnetic field, $\varepsilon \sim 1/(2\mathrm{Ha})^{1/2}$ in the case of large Hartmann numbers. In this experiment the error in measuring the velocity outside the boundary layers was 5%. For flows

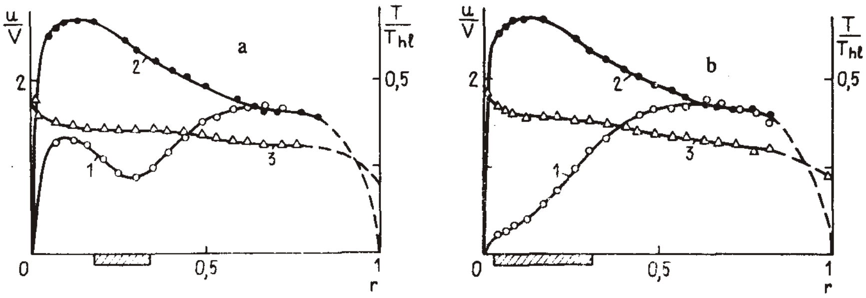

Fig. 2. Profiles of the mean velocity with (1) and without (2) short inserts on the channel bottom and of the temperature (3) with these inserts. The temperature of the heated wall with a laminar flow is T_{hl} = 28.94°C, Re = 28,200, and Ha = 600 (a); same with (b, curves 1 and 3) and without (curve 2) long inserts.

created by a longitudinal pressure gradient the factor in front of the brackets in the expression for v should be replaced by

$$-[(1+\alpha)/(\sigma B^2)][(\partial p)/(\partial x)].$$

In this case the root mean square error is $\zeta_p \sim [\alpha^2 + 1/(2\mathrm{Ha})]^{1/2}$.

A thermocouple (whose sensitive element has a diameter of 0.3 mm) was mounted in the anemometer probe 5 mm (along the magnetic field lines) from the point where the velocity was being measured in order to measure the locally averaged temperature of the liquid and the low-frequency temperature fluctuations. This location for the thermocouple is acceptable since at these magnetic fields the velocity and temperature distributions in the flow are uniform in the direction of the magnetic field lines.

The Nusselt number was determined by measuring the temperature difference between the hot and cold walls using thermocouples whose sensitive elements were positioned in holes 0.2 mm from the surfaces washed by the flow in the side walls of the channel and 35 mm from the bottom. In order to improve the thermal contact of the thermocouples with the walls the holes were filled with transformer oil. The thermocouples were made of 0.25-mm-diameter copper and constantan wires.

In analyzing the experimental data we have used the following dimensionless variables: the Reynolds number Re = $(b/\nu)(B\cdot I/(2\rho a))^{1/2}$ (where $2a$ is the height of the channel, $b = b_0 \ln(R_0/r_0)$ is the modified channel width, and b_0 is the distance between the side walls of the channel); the modified Hartmann number Ha = $(b/2a)Bb(\sigma/\mu)^{1/2}$; the ratio Rh = Re/Ha which characterizes the instability of the flow; and, the Nusselt number Nu = $\alpha b/\lambda$ with $\alpha = W/[F(T_h - T_c)/2]$ (where W is the thermal flux through the surface area $F = 4\pi r_0 a$, T_h and T_c are the temperatures of the hot and cold side walls, and λ is the thermal conductivity of the liquid). The mean and fluctuating velocities were converted to dimensionless form with respect to the mean divergent velocity $V = [BI/(2\rho a)]^{1/2}$ and the temperature fluctuations, with respect to $\Delta T = T_h - T_c$. The velocity and temperature characteristics were measured radially in the midplane between two adjacent inserts.

2. Results and Discussion. It is clear from the velocity distributions shown in Fig. 2a that when short conducting inserts are present, a nonuniform flow develops in the channel similar to the flow in the wake behind a body with a velocity minimum behind an insert (curve 1) while in a channel with a nonconducting bottom the flow is similar to the flow in a homopolar device with a velocity maximum near the heated wall (curve 2).

Since the readjustment of the flow in a strong magnetic field is greatest in the plane perpendicular to the field, we shall consider the equation for the corresponding component of the vorticity,

$$(\mathrm{v}\nabla)\omega_z = \nu\Delta\omega_z + B_z \partial j_z/\partial z.$$

This implies that, even in a nonviscous flow, a component of the vorticity parallel to the magnetic field will appear when a nonpotential electromagnetic force is present.

The shorting of the electric current through the conductivity insert creates a nonuniform current distribution along the magnetic field at the boundary of the insert and this produces a vortical component of the electromagnetic force, $\mathrm{rot}_z(\mathbf{j} \times \mathbf{B}) = B_z \partial j_z/\partial z$, which facilitates the development, in this zone, of vorticity (in the flow) parallel to the field. In the case of Fig. 2a (curve 1), the components of the vorticity at the boundaries of the conducting insert r = 0.18 and r = 0.33 have different signs. Hence, the velocity distribution of this flow differs from that of a flow in a channel with an insulating bottom (Fig. 2a,

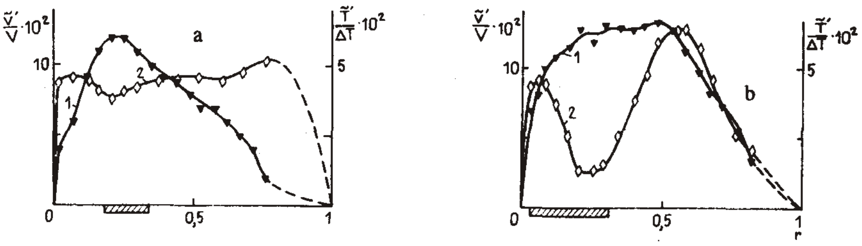

Fig. 3. Radial distributions of the intensities of fluctuations in the radial velocity (1) and temperature (2) in the presence of short (a) and long (b) inserts. T_{h1}, Re, and Ha are the same as in Fig. 2.

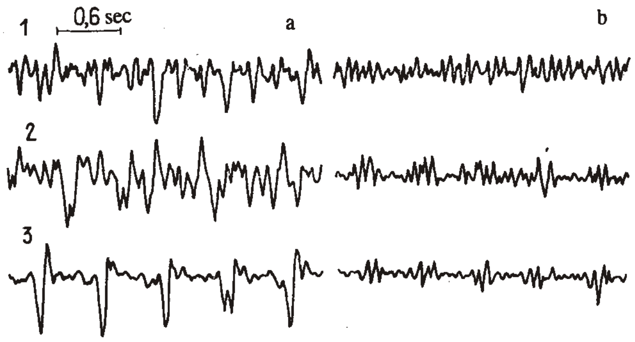

Fig. 4. Traces of the radial velocity fluctuations in a channel with long inserts: (1) $\tilde{v}'/V = 0.12$, $r = 0.15$; (2) $\tilde{v}'/V = 0.13$, $r = 0.24$; (3) $\tilde{v}'/V = 0.13$, $r = 0.42$; (a) without restriction as to frequency, (b) frequency components above 10 Hz.

curve 2). Stagnation zones that are stretched out along the magnetic field and are carried along by the liquid flow develop above the conducting inserts as a result of the vorticity.

Similar mechanisms for the evolution of the velocity structure show up in flows with long inserts positioned near the heated wall. The only difference is that at the end of an insert near the heated wall the vorticity is suppressed and the velocity profile has a single maximum (Fig. 2b, curve 1).

Temperature measurements across the channel with an insulating bottom at Rh = 42.73 showed that there is a large temperature gradient for $r = 0.05$-0.25, so that the temperature of the hot wall is only 8% lower than in the case of a laminar flow, while the heat transfer coefficient (as will be shown below) increases by a factor of 1.25. The small drop in the temperature of the hot wall during natural turbulence is explained by the low intensity (up to 3%) and small spatial scale of the perturbations generated in narrow zones with velocity shear near the heated wall (Fig. 2a and b, curves 2). Because of the small spatial scale of these perturbations, even in high magnetic fields they will continue to be essentially three-dimensional and, therefore, subject to strong Joule dissipation.

The temperature distributions shows in Figs. 2a and b (curves 3) indicate that the temperature of the liquid does not vary greatly across channels with either short or long inserts. This is explained by a substantial intensification of turbulent mixing of the liquid over essentially the entire width of the flow. Here the temperature of the heated wall is half that for a turbulent flow in the channel with an insulating bottom. This behavior of the temperature distribution is related to the strong instability of the flow as it flows around the stagnation zones which develop above the conducting inserts and to the generation of perturbations with substantial intensities. Large vortices develop on the shear of the mean velocity; these occupy a larger fraction of the flow cross section and facilitate equilibration of the temperature of the fluid over the channel cross section.

The distribution of the velocity fluctuations shown in Fig. 3a for a channel with short inserts confirms the existence in the channel of large scale vortices whose centers (to judge from the position of the peak intensity of the radial velocity fluctuations) are at $r \approx 0.25$. The asymmetry of the distribution of the fluctuations in the velocity with respect to the maxi-

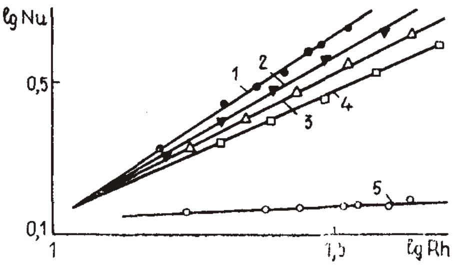

Fig. 5. The Nusselt number as a function of Rh when short and long inserts are present with Ha = 660 (1), 565 (2), 471 (3), and 396 (4), a well as when no inserts are present with Ha = 660 (5).

mum indicates that the walls have an effect on the shape of the vortices and their deformation. The existence of large scale vortical structures in the flow is also suggested by the intensity distribution of the temperature fluctuations. They remain high over almost all the channel width.

Figure 3b demonstrates the difference in the distributions of the fluctuations in velocity and temperature for a channel with long inserts. Since here the vortices detach on one side near the stagnation zones, the fluctuations in the radial velocity remain strong across half the channel width while the profile of the temperature fluctuations has a distinct M-shape.

Note that these temperature fluctuation profiles, which are similar to the profiles of the fluctuations in the azimuthal velocity, as well as the boundaries of the profile of the radial velocity fluctuations, provide a fairly reliable estimate of the transverse dimensions of the vortices. Thus, the outer boundaries of the vortices in the radial direction lie at r = 0.05-(0.6-0.8) for the two cases considered here. Observations of the free surface of the flow when the upper cover is removed confirm this conclusion.

The traces of radial velocity fluctuations shown in Fig. 4 for a flow in a channel with long inserts show that the bulk of the energy in the fluctuating motion is concentrated in large-scale vortices. Near the heated wall at a distance of r = 0.15 the contribution to the frequency spectrum from high-frequency velocity fluctuations is greater than at the other two positions. Filtering out the low-frequency part of the velocity fluctuations (traces on the right) shows that the range of frequencies corresponding to the large-scale vortices lies in the interval Δf = 0-10 Hz.

The presence in the flow of large-scale two-dimensional vortical structures should lead to a substantial rise in heat loss from the heated wall and to an increase in the heat transfer coefficient over the cross section of the flow. For comparison Fig. 5 shows data for flows in channels with and without conducting inserts. It is clear that these two cases differ substantially. Within the range of Hartmann numbers studied here, if large-scale vortical structures are excited then the Nusselt number increases by several times at large Ha (curves 1-4) compared to the case when no vortical structures are present (curve 5). A high magnetic field corresponds to a higher slope of the lines. Note that the dependence of the Nusselt number on Rh has a power law form for different values of the Hartmann number. For Rh = 12.6-42.73 these dependences can be written in the form $Nu \propto Rh^n$, where the exponent depends on Ha. In the case of vortical flows all the lines intersect at the point Rh = Rh_{cr} = 12.6, where Nu = 1.5. In laminar flows (Rh < 12.6) the Nusslet number remains constant at 1.2.

Studies of the stability limits of flows for both types of inserts showed that when Rh = 12.6 the flow loses stability as it flows around the stagnation zones and when Rh > 12.6 vortical perturbations of substantial intensity develop (see Fig. 3a and b).

The existence of a single value of Rh_{cr} for different values of Ha shows that the parameter Rh determines the stability boundary for a given type of flow.

Figure 5 also shows that for fixed Rh > Rh_{cr}, as Ha increases the transfer of energy from the mean motion to the vortical motion predominates over friction of two-dimensional vortices at walls that are perpendicular to the field. As a result the transverse scale-length of the vortical perturbations increases and for certain values of Ha an equilibrium state develops between the input of energy to the vortical motion and its dissipation by vortices at walls perpendicular to the field. The increase in the transverse scale of the perturbations as the magnetic field is raised also ensure that the heat transfer coefficients will increase. On this basis, the Nusselt number calculated with the temperature of the cold wall for Rh = 42.73 and Ha = 660 is 5, while the Nusselt number calculated from the temperature of the flow core at r = 0.5 (Fig. 2a and b) is 7.8. In the case of a channel with a nonconducting bottom at Ha = 660, the Nusslet number only reaches 1.5 at Rh = 42.73

since heat transfer takes place through small-scale vortices and the function Nu = Nu(Rh) varies little over a wide range of Rh (curve 5).

Conclusions. The excitation of large-scale vortical structures oriented along the magnetic field in the flow makes it possible to intensify the heat transfer process by a factor of 5-6. The temperature distribution becomes uniform over almost the entire cross section of the flow despite a nonuniform velocity distribution.

Calculations show that the energy expenditure in this case is 5-6 times lower than the energy required to obtain velocities high enough to ensure the same rate of heat transfer in an insulated channel.

REFERENCES

1. Yu. B. Kolesnikov and N. N. Polyakov, "Experimental studies of an axisymmetric shear rotating flow in a uniform axial magnetic field. Mean flow and the intensity of velocity fluctuations," Magn. Gidrodin., No. 3, 83-89 (1983).
2. Yu. B. Kolesnikov, "Experimental studies of the instability of plane-parallel shear flows in a magnetic field," Magn. Gidrodin., No. 1, pp. 60-66 (1985).
3. A. A. Kljukin and Yu. B. Kolesnikov, "MHD instabilities and turbulence in liquid metal shear flow," in: Proc. IUTAM Symp. on Liquid Metal MHD, Riga (1988), Liquid Metal Magnetohydrodynamics, Kluwer Academic Publishers, Netherlands (1989), pp. 449-454.
4. Yu. B. Kolesnikov and A. B. Tsinober, "Magnetohydrodynamics flows in the neighborhood of a discontinuity in the conductivity at a wall," Magn. Gidrodin., No. 1, 70-74 (1972).
5. Yu. B. Kolesnikov, Two-dimensional turbulent flows in channels with nonuniform wall conductivity," Magn. Gidrodin., No. 3, 32-36 (1972).
6. R. A. Alpher, H. Hurwitz, R. H. Johnson, and D. R. White, "Some studies of free-surface mercury magneto-hydrodynamics," Rev. Mod. Phys., **32,** 758 (1960).
7. O. V. Andreev and Yu. B. Kolesnikov, "Heat transfer intensification in liquid metal flows using vortices," in: Abstracts of talks at the International Conf. on MHD Processes for the Protection of the Environment, Kiev, Odessa (1992), p. 241.